

## Effects of Disorder on Ferromagnetism in Diluted Magnetic Semiconductors

Mona Berciu and R. N. Bhatt

*Department of Electrical Engineering, Princeton University, Princeton, New Jersey 08544*

(Received 17 November 2000; published 21 August 2001)

We present results of a numerical mean-field treatment of interacting spins and carriers in doped diluted magnetic semiconductors, which takes into account the positional disorder present in these alloy systems. Within our mean-field approximation, disorder enhances the ferromagnetic transition temperature for metallic densities not too far from the metal-insulator transition. Concurrently, the ferromagnetic phase is found to have very unusual temperature dependence of the magnetization as well as specific heat as a result of disorder. Unusual spin and charge transport is implied.

DOI: 10.1103/PhysRevLett.87.107203

PACS numbers: 75.50.Pp, 71.30.+h, 75.40.Mg

Following the discovery of a ferromagnetic transition in  $\text{Ga}_{1-x}\text{Mn}_x\text{As}$  at temperatures in excess of 100 K [1–3], well above those found in counterparts based on II-VI semiconductors [4], there has been a surge in interest in the magnetic properties of diluted magnetic semiconductors (DMS). Theoretical models abound to explain the ferromagnetism [5–7]. While it is generally accepted that the ferromagnetism is due to an effective interaction between the magnetic ions (Mn) mediated by mobile carriers (holes, since Mn, a group II element substitutes for Ga, a group III element), different models differ in detail, e.g., whether the interaction is RKKY or not, and also the approximations used to model the system.

In nonmagnetic doped semiconductors, such as phosphorus doped silicon [8], there has been no evidence for ferromagnetism due to carriers. Indeed, carrier hopping at low doping concentrations in the insulating phase is known to induce antiferromagnetic interactions between localized states, leading to a valence-bond-glass-like state down to the lowest observable temperatures [9]. In contrast, ferromagnetic tendencies were detected in doped diluted II-VI magnetic semiconductors already in the insulating regime at low temperatures [10], and subsequently ferromagnetism was observed in both II-VI and III-V semiconductors at metallic doping densities.

In insulating DMS, the presence of Mn has been shown [11,12] to overwhelm the antiferromagnetic interaction between charge carriers, leading to an essentially ferromagnetic ground state. Monte Carlo simulations [13] for II-VI DMS in the insulating phase show that the ferromagnetic phase is very unusual, with a highly inhomogeneous magnetic profile, leading to unconventional properties such as  $M(T)$  curve that is not described by expansions around the critical point (critical point theories) or zero temperature (spin wave theories) over most of the ferromagnetic phase. By contrast, theoretical models for the metallic regime [5,6] have been based on the homogeneous electron gas, with a few exceptions, such as the possibility of phase separation [7].

It is well known in conventional doped semiconductors that the carrier wave functions are those derived from an impurity band, for densities in the vicinity of the metal-insulator transition (MIT), up to a factor of 3–5 above the MIT density,  $n_c$  [14]. Density functional calculations [15] for a lattice of hydrogen atoms show this clearly. The variation of critical density with uniaxial stress in doped Si and Ge [16] is in agreement with calculations based on impurity band wave functions [17]. Local moments are known to dominate the low temperature behavior in doped semiconductors well into the metallic phase [8,18], and the effect is enhanced for compensated systems [19]. Raman measurements [20] in doped Si and infrared spectra [21] in GaAs also show features in the metallic phase characteristic of the impurity wave function.

Ferromagnetism is found in  $\text{Ga}_{1-x}\text{Mn}_x\text{As}$  not far from a MIT, with insulating behavior seen both at low and high Mn concentration [22]. Further, the system is heavily compensated [22–24] with a carrier density only around 10% the Mn density. (Mn is nominally an acceptor in GaAs and is expected to donate one hole per Mn.) The vicinity of the MIT, and the large compensation, which implies large disorder, motivate studying a model that takes into account disorder as well as the impurity potential at the outset, to see what their effects are on the magnetic properties of the system.

Given the added complications of disorder, we study a model based on an impurity band of hydrogenic centers with spin-1/2 (instead of the more complex  $s = 3/2$  wave functions appropriate for acceptors), coupled to localized Mn  $d$  electrons in their  $S = 5/2$  ground state. The  $s = 3/2$  case, while technically more complicated, should yield qualitatively similar conclusions. The impurity band is described in terms of a tight binding Hamiltonian of the ground state impurity wave functions at the impurity sites, which are distributed randomly on the Ga sites [25]. As in previous work [11,13], the carriers are coupled to the Mn spins by an antiferromagnetic (AFM) Heisenberg exchange interaction. The Hamiltonian we study is thus

$$\mathcal{H} = \sum_{i,j} t_{ij} c_{i\sigma}^\dagger c_{j\sigma} + \sum_{i,j} J_{ij} \vec{S}(i) \left( c_{j\alpha}^\dagger \frac{1}{2} \vec{\sigma}_{\alpha\beta} c_{j\beta} \right) - g \mu_B H \sum_i \frac{\sigma}{2} c_{i\sigma}^\dagger c_{i\sigma} - \tilde{g} \mu_B H \sum_i S^z(i). \quad (1)$$

Here,  $\vec{R}_i$  ( $i = 1, N_d$ ) denotes the random positions of the Mn impurities, and  $c_{i\sigma}^\dagger$  is the creation operator of a hole with spin  $\sigma$  in the bound state associated with the  $i$ th Mn impurity. The first term in Eq. (1) describes the hopping of holes between various sites, with the hopping matrix  $t_{ij} = t(|\vec{R}_i - \vec{R}_j|)$  given by  $t(r) = 2(1 + r/a_B) \exp(-r/a_B) \text{Ry}$  [17], where the Ry is the binding energy of the hole,  $E_b$ , and  $a_B = \epsilon \hbar^2 / m^* e^2$  is the hydrogenic Bohr radius. The second term is the AFM interaction between Mn spins  $\vec{S}(i)$  and hole spins. Since Mn spins are strongly localized, the exchange integral is simply given by  $J_{ij} = J \exp(-2|\vec{R}_i - \vec{R}_j|/a_B)$ , reflecting the probability of finding the hole in the impurity state around  $j$  on the  $i$ th Mn spin. The last line in Eq. (1) describes interactions with an external magnetic field  $H$ .

We study finite size lattices containing  $L^3$  simple cubic unit cells (lattice constant  $a$ ) of the zinc-blende structure.  $N_d$  of the Ga fcc sublattice are substituted at random by Mn, leading to a Mn concentration  $n_{\text{Mn}} = 4x/a^3$ , where  $x = N_d/4L^3$ . The total number of holes is  $N_h = pN_d$ , implying a hole concentration  $n_h = pn_{\text{Mn}}$ . In all simulations presented in this paper we choose  $L$  such that for the corresponding  $x$  and  $p$ , we have  $N_h > 50$  and  $N_d > 500$ , so as to minimize finite size effects. Thus, in the absence of external magnetic fields, the problem can be scaled in terms of four dimensionless parameters:  $J/E_b$ ,  $a_B/a$ ,  $n_h a_B^3$ , and  $x$ .

In this paper, we use parameters believed to be appropriate for  $\text{Ga}_{1-x}\text{Mn}_x\text{As}$ : lattice constant  $a = 5.65 \text{ \AA}$ , hole binding energy  $E_b = 112.4 \text{ meV} = 1 \text{ Ry}$  [26], with a consequent Bohr radius (in our model) of  $a_B = 7.8 \text{ \AA}$  [27], and an exchange integral  $J = 15 \text{ meV}$  [28]. Typical values of the Mn and hole concentrations are  $x = 0.01\text{--}0.05$  and  $p = 5\%\text{--}10\%$  [23,24]. A more comprehensive study, including a number of effects left out of this model, is being completed [29]. With these parameters, the typical hopping parameter is  $t(4a_B) = 20 \text{ meV}$ , though it should be emphasized that  $t_{ij}$  are distributed over a wide range [29].

We treat the AFM interaction within the mean-field approximation (MFA), which leads to the replacement  $\vec{S}(i) \hat{s}_j \rightarrow \langle \vec{S}(i) \rangle \hat{s}_j + \vec{S}(i) \langle \hat{s}_j \rangle - \langle \vec{S}(i) \rangle \langle \hat{s}_j \rangle$ , where  $\hat{s}_j = c_{j\alpha}^\dagger \frac{1}{2} \vec{\sigma}_{\alpha\beta} c_{j\beta}$ . The charge carrier Hamiltonian now contains the hopping term and an effective on-site interaction  $\sum_j \epsilon_{\alpha\beta}(j) c_{j\alpha}^\dagger c_{j\beta}$ , with  $\epsilon_{\alpha\beta}(j) = \frac{1}{2} \sum_i J_{ij} \vec{\sigma}_{\alpha\beta} \langle \vec{S}(i) \rangle$ , and can be numerically diagonalized for any configuration  $\langle \vec{S}(i) \rangle$  of the Mn spins, allowing the calculation of the charge carrier spin expectation values  $\langle \hat{s}_j \rangle$ . In turn, these allow us to compute the new expectation values for the

Mn spins,  $|\langle \vec{S}(i) \rangle| = \mathcal{B}_S(\beta H_i)$ ,  $\langle \vec{S}(i) \rangle \parallel \vec{H}_i$ , where  $\vec{H}_i = -\sum_j J_{ij} \langle \hat{s}_j \rangle$  and  $\mathcal{B}_S(x)$  is the Brillouin function.

The process is repeated until self-consistency is reached at each site [29]. As usual in MFA, the symmetry to spin rotations is spontaneously broken and the expectation values are nonzero for some direction, which we choose as the  $z$  axis (this is equivalent to having an infinitesimally small magnetic field). The average contributions to the total magnetization of the Mn and hole spins are then proportional to  $S_{\text{Mn}} = 1/N_d \sum_i \langle S^z(i) \rangle$  and  $s_h = 1/N_h \sum_i \langle \hat{s}_i^z \rangle$ . As might be expected, below a temperature  $T_c$ , the system develops nonzero expectation values for the Mn and hole magnetizations, through hole-induced alignment of the Mn spins. In Fig. 1 we show the average Mn and hole spins as a function of temperature,  $T$ , for a system with  $x = 0.00926$  and  $p = 10\%$ , for a typical random Mn distribution (full lines). For comparison, we also show the corresponding results (dashed lines) for a system with the same Mn concentration, but with Mn ions arranged on a simple cubic lattice, with a (super)lattice constant  $a_L = a/(4x)^{1/3} = 3a$ . Because of their AFM interaction, the two expectation values have opposite signs, with the Mn spin saturating at  $\frac{5}{2}$  and the hole spin saturating at  $-\frac{1}{2}$  at low temperatures. [The total magnetization  $M(T)$  of the system has a  $T$  dependence similar to that of  $S_{\text{Mn}}$ , since Mn spins outnumber holes ten to one, and also have a higher moment].

The first observation is that the magnetization of the disordered system does not have the Brillouin-function shape typical for uniform ferromagnets. This is in part due to the small carrier density relative to the Mn spin density; however, an even greater effect comes from the wide distribution of exchange couplings and hopping integrals, because of which many Mn spins do not order down to extremely low  $T$ . This is made clear in the inset for Fig. 1, which compares the specific heat for the two configurations on

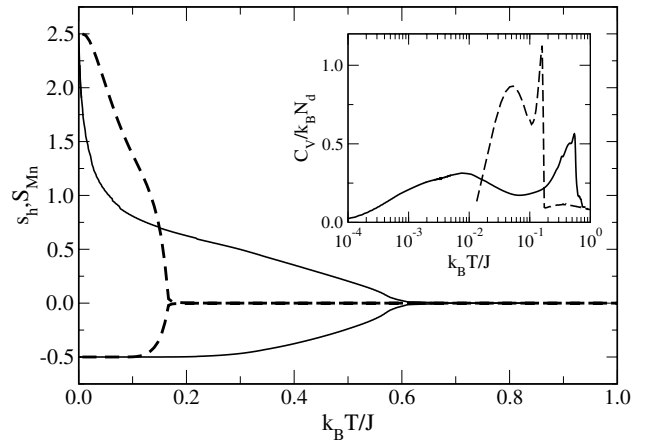


FIG. 1. The average Mn spin  $S_{\text{Mn}}$  ( $> 0$ ) and the average spin per hole  $s_h$  ( $< 0$ ) for a typical random Mn distribution (full lines) and a simple cubic ordered Mn distribution (dashed lines), both for  $x = 0.00926$  and  $p = 10\%$  (see text). The inset shows the corresponding specific heats per Mn spin.

a logarithmic scale for  $T$ : the disordered case shows a pronounced peak at temperatures *well* below  $T_c$ , and significantly below its lattice counterpart. Further, we find that the average Mn moment at  $T = 0.2T_c$  is well below the saturation value of  $5/2$ , in accord with experimental data [23], but in contrast with results obtained from homogeneous electron gas models.

A second, surprising result is that randomness in the Mn positions leads to a significant increase in  $T_c$ . This is because, in the disordered system, holes prefer regions of higher local concentration of Mn, where they lower their total (magnetic and kinetic) energy, by polarizing the Mn spins and hopping among several nearby Mn sites. As a result, these regions of higher Mn concentration become spin polarized at higher temperatures than in the uniform system, and the resultant  $T_c$  is increased. This is similar to a percolationlike situation. We caution that this increase may be significantly overestimated in a MFA such as ours, since spin fluctuations between weakly coupled polarized clusters are not treated accurately.

On the other hand, in a disordered system, the lower density Mn regions have a lower than average probability to be visited by the holes, and as a result the Mn spins in these regions only align ferromagnetically at extremely low temperatures (see Fig. 1); such an effect is probably well captured by our scheme. We would like to emphasize the fact that the holes at the Fermi energy at the densities studied are either itinerant, or close to being so. An analysis of hole wave functions [29] shows this delocalization, along with the higher weight of holes in the regions of high Mn concentration. This delocalization is responsible for alignment of the polarization at these high temperatures (relative to the insulating system [13]). Holes traveling between various high-density regions force the alignment of Mn spins in each region to be the same, in order to minimize their kinetic energy.

This picture can be checked by “tuning” the amount of disorder (randomness) in the Mn positions. In Fig. 2 we show the average hole and Mn spins curves, for four types of Mn distributions, with  $x = 0.00926$  and  $p = 10\%$ . In order of increasing  $T_c$ , they are (a) an ordered Mn cubic superlattice; (b) weak disorder, corresponding to randomly displacing each Mn in (a) to one of the 12 nearest-neighbor sites of the underlying fcc sublattice; (c) moderate disorder, corresponding to a random distribution of Mn on the fcc sublattice, subject to a constraint that all Mn-Mn distances are greater than  $2a$ ; (d) completely random distribution of Mn on the fcc sublattice. With increasing randomness,  $T_c$  increases, while saturation of  $M(T)$  is simultaneously pushed to lower  $T$ . The sensitivity to disorder suggests that carrier density is not the only parameter characterizing the ferromagnetic behavior in DMS; indeed, since original submission of this manuscript, changes in  $M(T)$  curves with annealing time have been seen experimentally [30].

We find a qualitatively similar picture holds for higher Mn concentrations as well as higher hole densities, though the effects are quantitatively less. (Our model, which

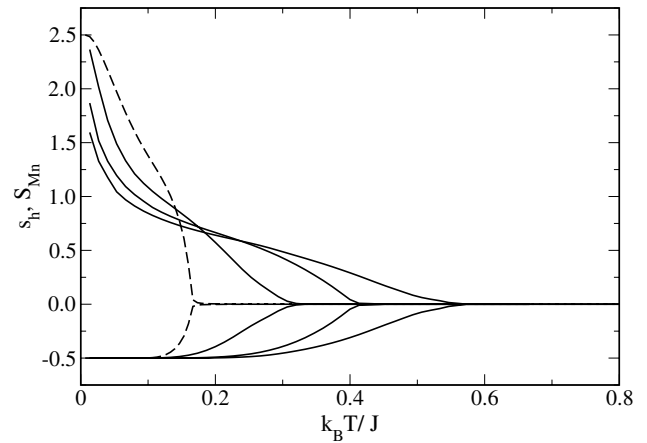


FIG. 2. The average Mn spin  $S_{Mn}$  and average spin per hole  $s_h$  for doping concentration  $x = 0.00926$  and  $p = 10\%$ . In increasing order of  $T_c$ , the curves correspond to ordered, weakly disordered, moderately disordered, and completely random distributions of Mn (see text).

does not include band states, is likely to be less accurate at high densities.) In Fig. 3 we show the Mn and hole spins for both the simple cubic superlattice and the random Mn distribution on the fcc sublattice for  $x = 0.05$  for two different  $p$ . While  $T_c$  is again larger in the random system in MFA, the percentage increase is smaller than in the  $x = 0.00926$  case. Increasing the hole concentration from  $p = 10\%$  to  $p = 30\%$  makes the curves more Brillouin-like. This is because the fluctuations in the local doping are smaller at higher Mn concentrations, and increased hole doping further reduces the width of the exchange distribution.

Our model, being based on the low doping limit, likely overestimates the role of disorder; however, because ferromagnetism in DMS is seen at low doping densities, not too far from the metal-insulator transition, our work does strongly suggest that models based on the homogeneous

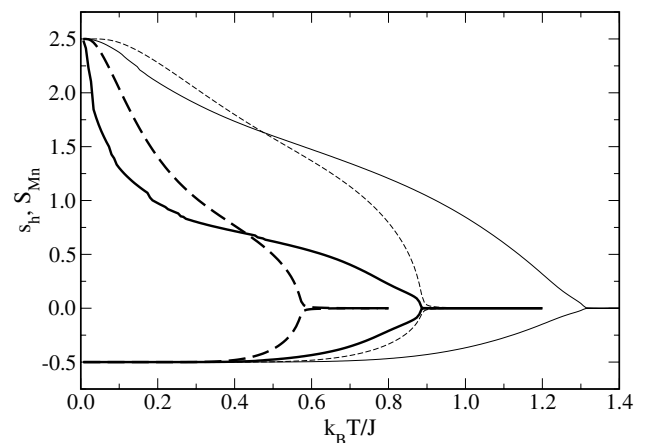


FIG. 3. The average Mn spin  $S_{Mn}$  and the average spin per hole  $s_h$  for doping concentration  $x = 0.05$  and  $p = 10\%$  (thick lines) and  $30\%$  (thin lines) for typical random Mn distributions (full lines) and simple cubic ordered Mn distributions (dashed lines).

electron gas (whether mean field [6], or with perturbative RKKY exchange [5]) will not correctly capture the nature of ferromagnetism. In particular, it casts doubt on their quantitative fits to the observed  $T_c$  in  $\text{Ga}_{1-x}\text{Mn}_x\text{As}$ . Our calculation, while including the random positions of the Mn dopants, leaves out disorder effects due to compensation, as well as fluctuation effects left out in the MFA. At higher Mn concentrations, direct Mn-Mn interactions (which are needed to account for spin-glass-like behavior seen in many II-VI DMS above 20% Mn) become important, while for higher hole concentrations, one may have to include the band states in addition to the impurity band, and possibly Coulomb interactions between carriers as well. While these will have quantitative effects on the results [31], the unusual shape of the magnetization curve and thermodynamic properties is likely to remain at low doping, judging from the results of numerical Monte Carlo simulations for the insulating phase of doped DMS [13]. Local experimental probes such as ESR and NMR would be especially valuable in ascertaining any inhomogeneities in the magnetization and carrier density profile, and help uncover the nature of ferromagnetism in doped DMS at these low carrier densities.

In conclusion, the nature of ferromagnetism in doped DMS for low doping, not too far above the metal-insulator transition density, is strongly affected by disorder, which may, surprisingly, aid higher  $T_c$  in this regime. Further, by appropriate tuning of various parameters, one may tailor the magnetic behavior  $M(H, T)$  in a manner not possible in simple uniform magnets [32]. This versatility makes DMS ferromagnetism near the MIT a very interesting problem from a theoretical point of view. Adding to the richness are possible effects of direct Mn-Mn interactions in concentrated systems (which lead to spin-glass behavior in undoped II-VI DMS [33]), the existence of a ferromagnetic metal-insulator transition (unlike conventional doped semiconductors and amorphous alloys), and the likely unusual electron and spin transport characteristics because of disorder.

This research was supported by NSF DMR-9809483. M.B. acknowledges support from NSERC, Canada. R.N.B. acknowledges the hospitality of the Isaac Newton Institute for Mathematical Sciences and of the Aspen Center for Physics while this research was ongoing.

- 
- [1] H. Ohno *et al.*, Appl. Phys. Lett. **69**, 363 (1996).  
 [2] M. Tanaka *et al.*, J. Cryst. Growth **175**, 1063 (1997).  
 [3] A. Van Esch *et al.*, Phys. Rev. B **56**, 13 103 (1997).  
 [4] A. Haury *et al.*, Phys. Rev. Lett. **79**, 511 (1997).  
 [5] T. Dietl *et al.*, Phys. Rev. B **55**, R3347 (1997); T. Jungwirth *et al.*, Phys. Rev. B **59**, 9818 (1999); T. Dietl *et al.*, Science **287**, 1019 (2000).  
 [6] J. König *et al.*, Phys. Rev. Lett. **84**, 5628 (2000).  
 [7] E. L. Nagaev, Phys. Status Solidi B **186**, 9 (1994); Phys. Usp. **38**, 497 (1995); **39**, 781 (1996).

- [8] M. A. Paalanen *et al.*, Phys. Rev. Lett. **61**, 597 (1988); M. A. Paalanen *et al.*, Physica (Amsterdam) **169B**, 223 (1991).  
 [9] R. N. Bhatt and P. A. Lee, Phys. Rev. Lett. **48**, 344 (1982).  
 [10] J. Z. Liu *et al.*, Bull. Am. Phys. Soc. **39**, 402 (1994).  
 [11] P. A. Wolff *et al.*, J. Appl. Phys. **79**, 5196 (1996); A. C. Durst, R. N. Bhatt, and P. A. Wolff (unpublished).  
 [12] D. Angelescu and R. N. Bhatt, cond-mat/0012279.  
 [13] Xin Wan and R. N. Bhatt, cond-mat/0009161.  
 [14] H. Fritzsche, in *The Metal Non-Metal Transition in Disordered Systems*, edited by L. R. Friedman and D. P. Tunstall (SUSSP, Edinburgh, 1978); N. F. Mott, J. Phys. (Paris) **50**, 2811 (1989); M. N. Alexander and D. F. Holcomb, Rev. Mod. Phys. **40**, 815 (1968).  
 [15] J. H. Rose *et al.*, Phys. Rev. B **21**, 3037 (1980).  
 [16] M. A. Paalanen *et al.*, Phys. Rev. Lett. **51**, 1896 (1983).  
 [17] R. N. Bhatt, Phys. Rev. B **24**, 3630 (1981); **26**, 1082 (1982).  
 [18] H. Alloul *et al.*, Phys. Rev. Lett. **59**, 578 (1987).  
 [19] M. J. Hirsch *et al.*, Phys. Rev. Lett. **68**, 1418 (1992).  
 [20] K. Jain *et al.*, Phys. Rev. B **12**, 5448 (1976).  
 [21] S. Liu *et al.*, Phys. Rev. B **48**, 11 394 (1993).  
 [22] H. Ohno, J. Magn. Magn. Mater. **200**, 110 (1999).  
 [23] B. Beschoten *et al.*, Phys. Rev. Lett. **83**, 3073 (1999).  
 [24] F. Matsukura *et al.*, Phys. Rev. B **57**, R2037 (1998).  
 [25] Unlike  $\text{Ga}_{1-x}\text{Mn}_x\text{As}$ , where the hydrogenic centers are located at the Mn spin sites, in II-VI semiconductors the carrier dopants and Mn spins are independently distributed, leading to substantial quantitative differences.  
 [26] A. K. Bhattacharjee and C. Benoit á la Guillaume, Solid State Commun. **113**, 17 (2000).  
 [27] Using the heavy hole effective mass in the spherical approximation to the Luttinger Hamiltonian  $m_h = m_e/[\gamma_1 - (6\gamma_3 + 4\gamma_2)/5] = 0.56m_e$  where for GaAs  $\gamma_1 = 7.65$ ,  $\gamma_2 = 2.41$ ,  $\gamma_3 = 3.28$  (see Bhattacharjee and Guillaume above), the Bohr radius of the impurity is  $a_B = \hbar/\sqrt{(2m_h E_b)} = 7.8 \text{ \AA}$  [B. I. Shklovskii and A. L. Efros, *Electronic Properties of Doped Semiconductors* (Springer-Verlag, Berlin, 1984)]. This agrees with the hydrogenic model result for the hole, for which  $a_B = e^2/(2\epsilon E_b) = 7.82 \text{ \AA}$ , using  $\epsilon = 10.66$  [26]. While this good agreement is likely fortuitous, similar values ( $a_B \approx 10 \text{ \AA}$ ) have been used in literature [see Van Esch *et al.* (Ref. [3])].  
 [28] The exchange integral is  $J = 3\epsilon$ , where  $\epsilon = 5 \text{ meV}$  is the value obtained in Ref. [26] for the AFM interaction of a hole with the spin of its impurity Mn. We include the factor of 3 as the simplest way to account for the fact that the heavy holes have spin projections  $j_z = \pm \frac{3}{2}$ , while in our model they are modeled as  $s_z = \pm \frac{1}{2}$  objects.  
 [29] Mona Berciu and R. N. Bhatt (unpublished).  
 [30] S. J. Potashnik *et al.*, cond-mat/0105541.  
 [31] For this reason, the numbers obtained in this paper are indicative of, but not directly comparable with, experiment.  
 [32] Uniform magnets as well as metallic alloys are characterized by deviations from a universal curve on a  $M(H, T)/M(0, 0)$  versus  $T/T_c$  and  $g\mu H/k_B T_c$  plot which are best described as weak ( $\leq 10-15\%$ ). [See T. Kaneyoshi, *Introduction to Amorphous Magnets* (World Scientific, Singapore, 1992), pp. 56-61.]  
 [33] See, e.g., S. Oseroff and P. H. Keesom, in *Diluted Magnetic Semiconductors*, edited by J. K. Furdyna and J. Kossut (Academic Press, New York, 1988).